

Belle and Belle II at TIFR

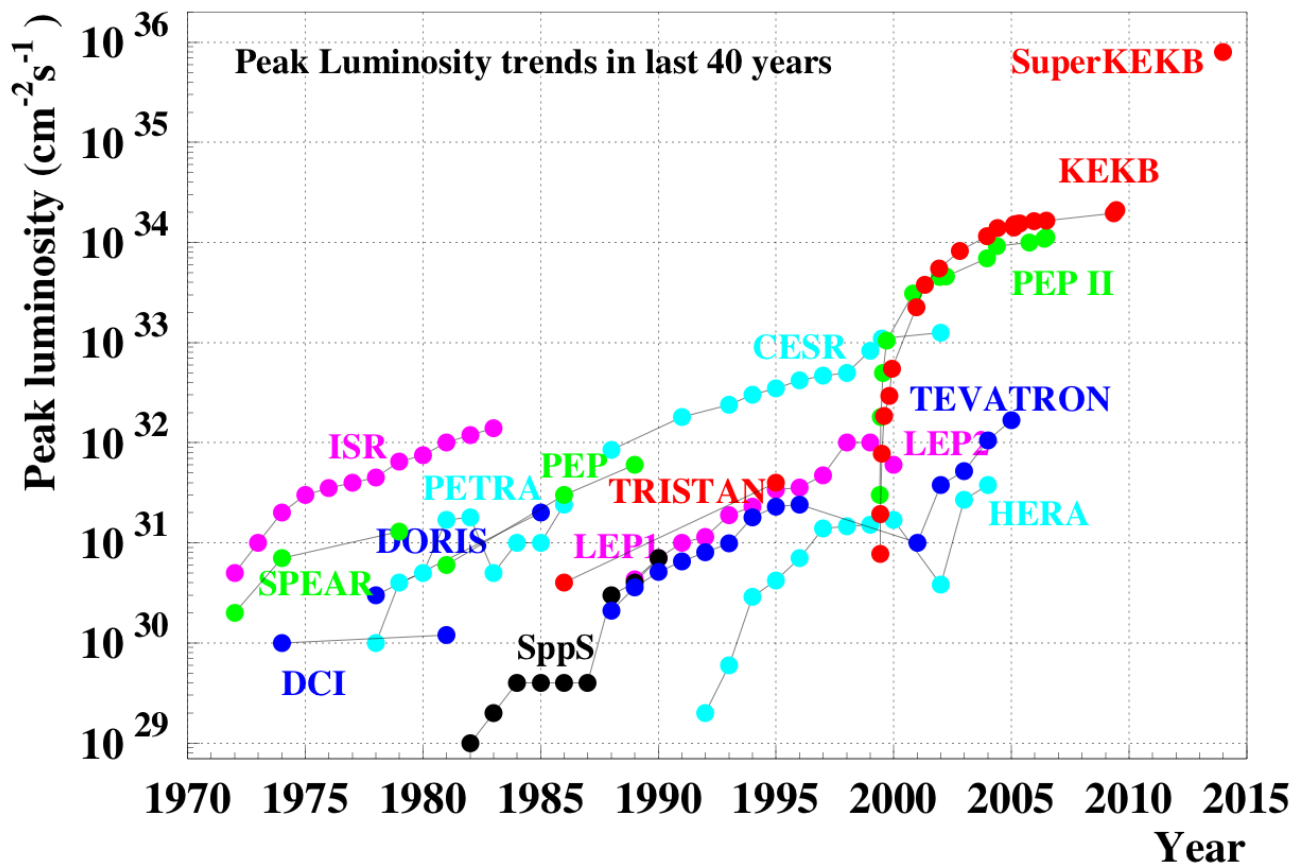


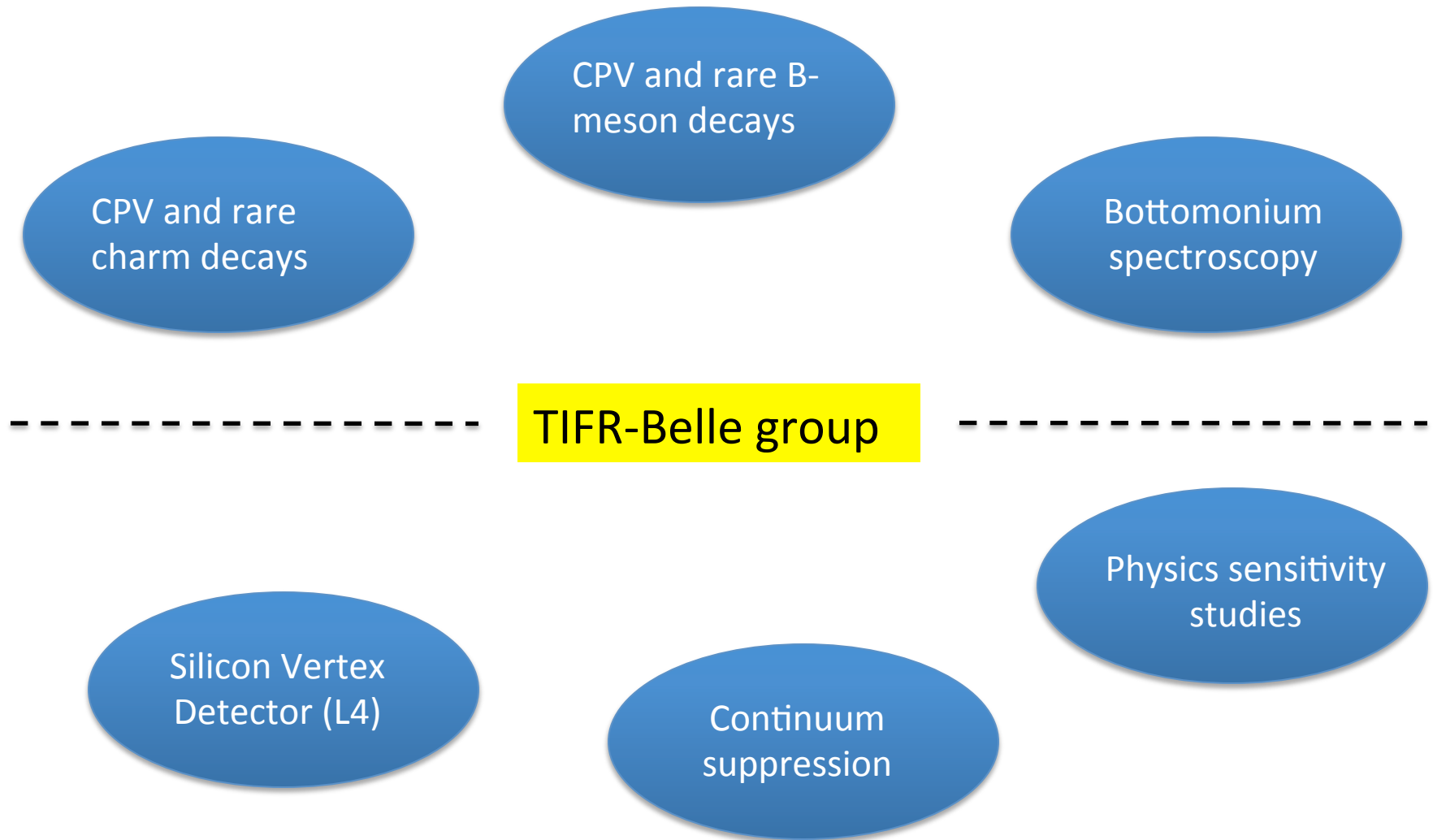
Gagan Mohanty



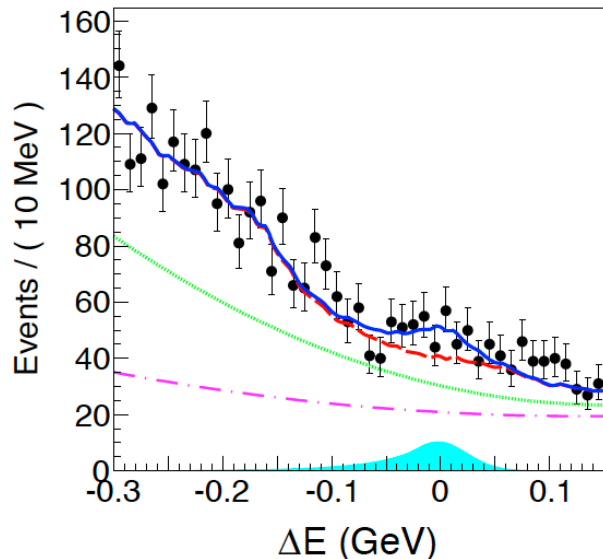
DHEP Annual Meeting @ TIFR
April 7-8, 2016

$$\Delta E \Delta t \sim 1$$





- A small group, having high visibility in terms of contribution and established leadership within the collaboration(s)



Evidence for the decay $B^0 \rightarrow K^+K^-\pi^0$

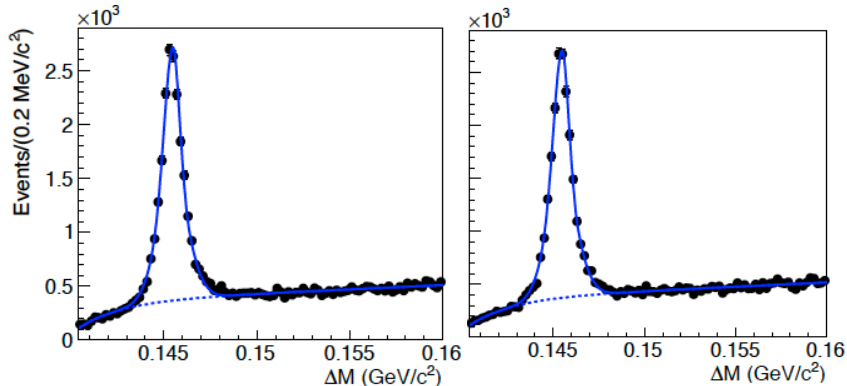
PRD 87, 091101(R) (2013)

- A challenging analysis challenged by huge continuum and peaking BB background
- Established a signal for the first time (3.5σ evidence)
- Will be a key analysis for Belle II

Measurements of Branching Fractions and Direct CP Asymmetries for $B \rightarrow K\pi, B \rightarrow \pi\pi$ and $B \rightarrow KK$ Decays PRD 87, 031103(R) (2013)

We report measurements of the branching fractions and direct CP asymmetries (\mathcal{A}_{CP}) for $B \rightarrow K\pi, \pi\pi$ and KK decays (but not $\pi^0\pi^0$) based on the final data sample of 772×10^6 $B\bar{B}$ pairs collected at the $\Upsilon(4S)$ resonance with the Belle detector at the KEKB asymmetric-energy e^+e^- collider. We set a 90% confidence-level upper limit for K^+K^- at 2.0×10^{-7} ; all other decays are observed with branching fractions ranging from 10^{-6} to 10^{-5} . In the $B^0/\bar{B}^0 \rightarrow K^\pm\pi^\mp$ mode, we confirm Belle's previously reported large \mathcal{A}_{CP} with a value of $-0.069 \pm 0.014 \pm 0.007$ and a significance of 4.4σ . For all other flavor-specific modes, we find \mathcal{A}_{CP} values consistent with zero, including $\mathcal{A}_{CP}(K^+\pi^0) = +0.043 \pm 0.024 \pm 0.007$ with 1.8σ significance. The difference of CP asymmetry between $B^\pm \rightarrow K^\pm\pi^0$ and $B^0/\bar{B}^0 \rightarrow K^\pm\pi^\mp$ is found to be $\Delta\mathcal{A}_{K\pi} \equiv \mathcal{A}_{CP}(K^+\pi^0) - \mathcal{A}_{CP}(K^+\pi^-) = +0.112 \pm 0.027 \pm 0.007$ with 4.0σ significance. We also calculate the ratios of partial widths for the $B \rightarrow K\pi$ decays. Using our results, we test the validity of the sum rule $\mathcal{A}_{CP}(K^+\pi^-) + \mathcal{A}_{CP}(K^0\pi^+) \frac{\Gamma(K^0\pi^+)}{\Gamma(K^+\pi^-)} - \mathcal{A}_{CP}(K^+\pi^0) \frac{2\Gamma(K^+\pi^0)}{\Gamma(K^+\pi^-)} - \mathcal{A}_{CP}(K^0\pi^0) \frac{2\Gamma(K^0\pi^0)}{\Gamma(K^+\pi^-)} = 0$ and obtain a sum of $-0.270 \pm 0.132 \pm 0.060$ with 1.9σ significance.

Search for CP violation in $D^0 \rightarrow \pi^0\pi^0$ decays

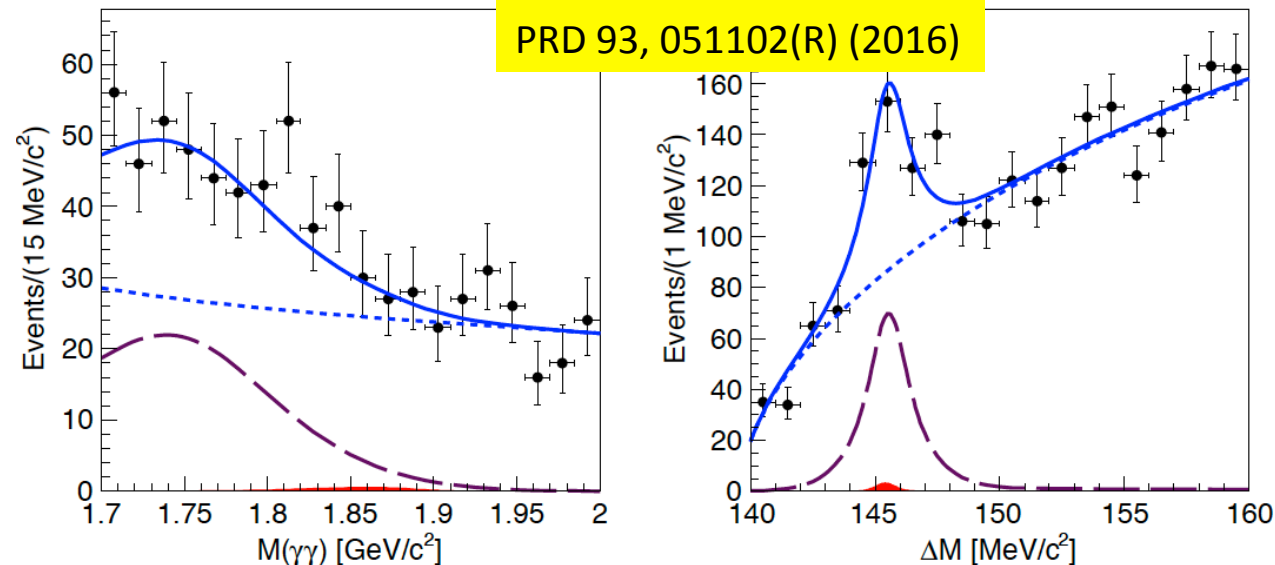


$$A_{CP}(D^0 \rightarrow \pi^0\pi^0) = (-0.03 \pm 0.64 \pm 0.10)\%$$

- Results consistent with no CP violation
- An order of magnitude improvement over the existing result

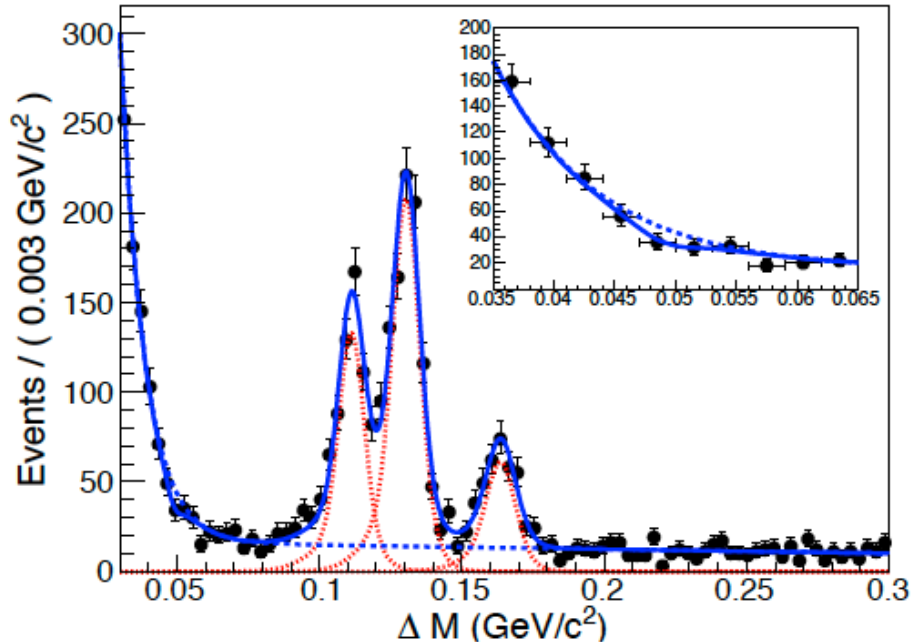
PRL 112, 211601 (2014)

Search for the rare decay $D^0 \rightarrow \gamma\gamma$



- A nice channel for NP, which can only be studied at e^+e^- flavor factories
- Set world's best limit (8.5×10^{-7}) in absence of a signal

Search for Bottomonium States in Exclusive Radiative $\Upsilon(2S)$ Decays

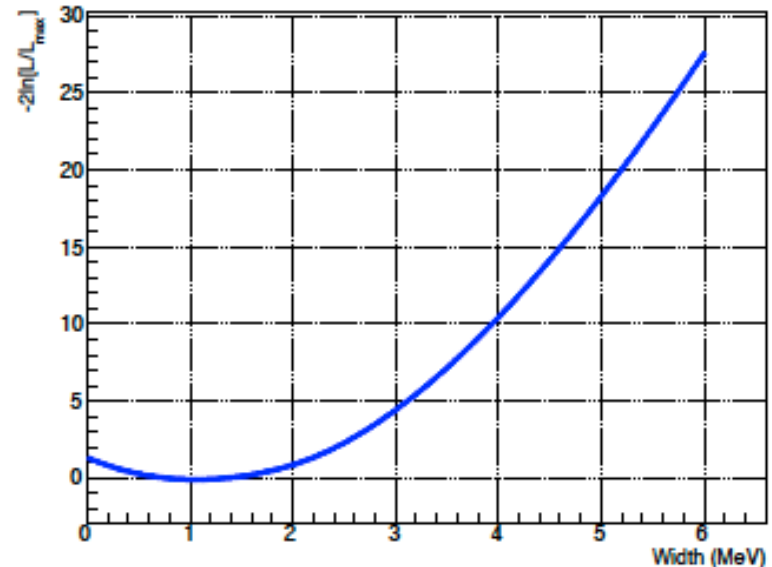


Paper in preparation

- ❑ 85 new decay channels of $\chi_{bj}(1P)$ are discovered
- ❑ First upper limit on the natural width of $\chi_{b0}(1P)$

PRL 111, 112001 (2013)

- ❑ Unambiguously refuted the claim of dubious $X_{bb}(9975)$ state, which was claimed by a study based on CLEO's data
- ❑ Paved way for further study on $\chi_{bj}(1P)$ states – see below

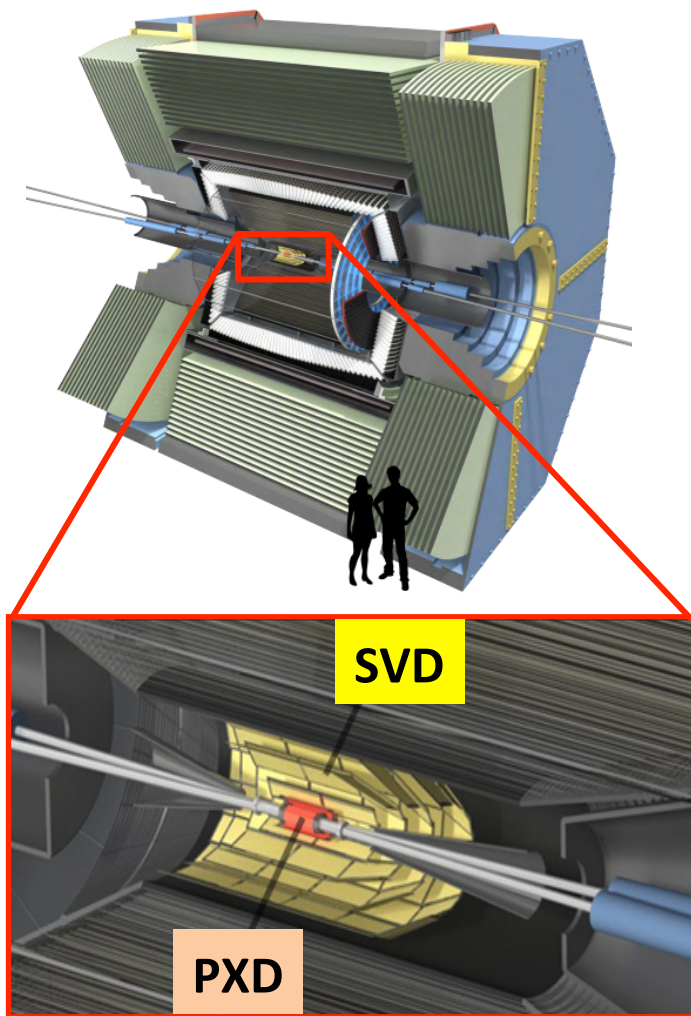


- Determine the vertex position of the weakly decaying particles
- Measure the two-dimensional track position and momentum for charged particles

- PiXeI Detector (PXD)
- Silicon Vertex Detector (SVD)
 - Double-sided silicon strip detectors (DSSDs)

VXD requirements

- Fast – to operate in high rate environment
- Excellent spatial resolution
- Radiation hard (up to 100 kGray)
- Good tracking capability – to track particles down to 50 MeV in p_T

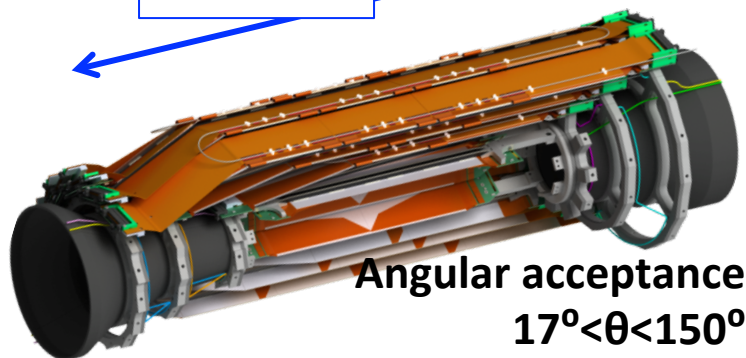


SVD Structure Overview

SVD cut model

~650mm

Backward



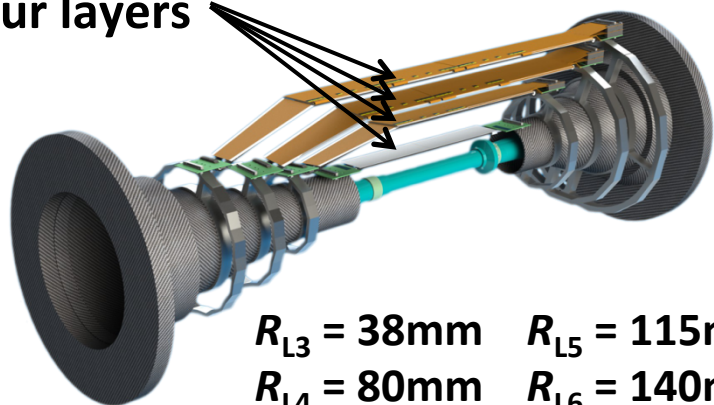
Angular acceptance
 $17^\circ < \theta < 150^\circ$

Forward

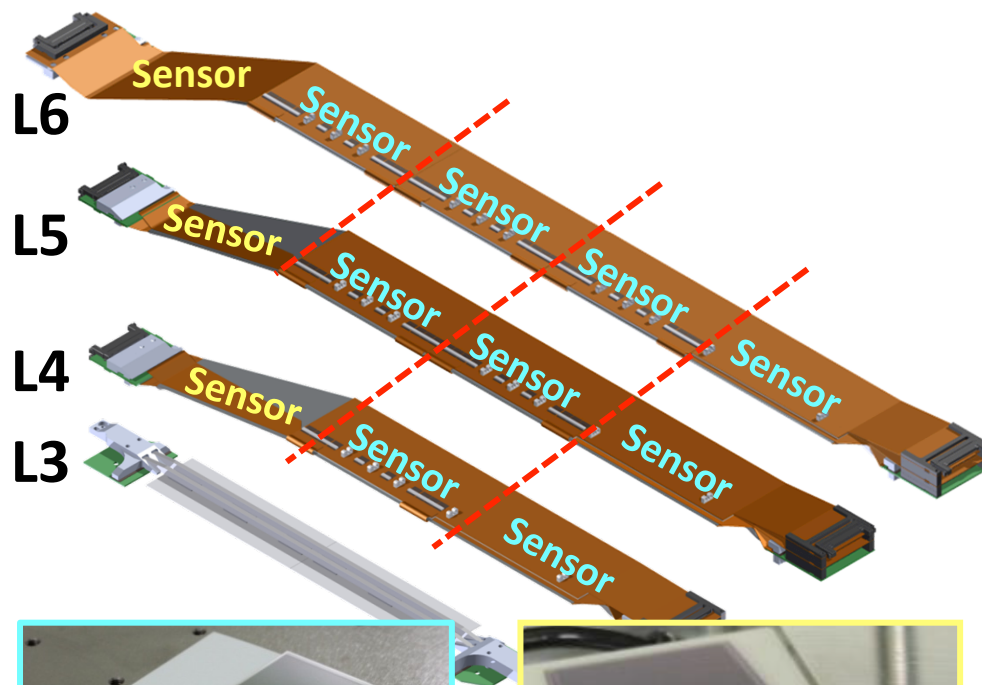
Layer	Institute
3	University of Melbourne
4	TIFR Mumbai
5	HEPHY Vienna
6	IPMU University of Tokyo
FW & BW	INFN Pisa

- 4 SVD layers (L3 to L6) composed of ladders arranged in a windmill structure
- Improved resolution at IP w.r.t Belle I
- Very lightweight – only $0.58\%X_0$ per layer

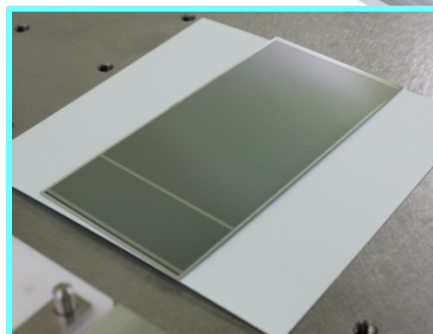
Four layers



$R_{L3} = 38\text{mm}$ $R_{L5} = 115\text{mm}$
 $R_{L4} = 80\text{mm}$ $R_{L6} = 140\text{mm}$



Layer	Ladders	Sensors / Ladder	APVs
6	16	5	800
5	12	4	480
4	10	3	300
3	7	2	168



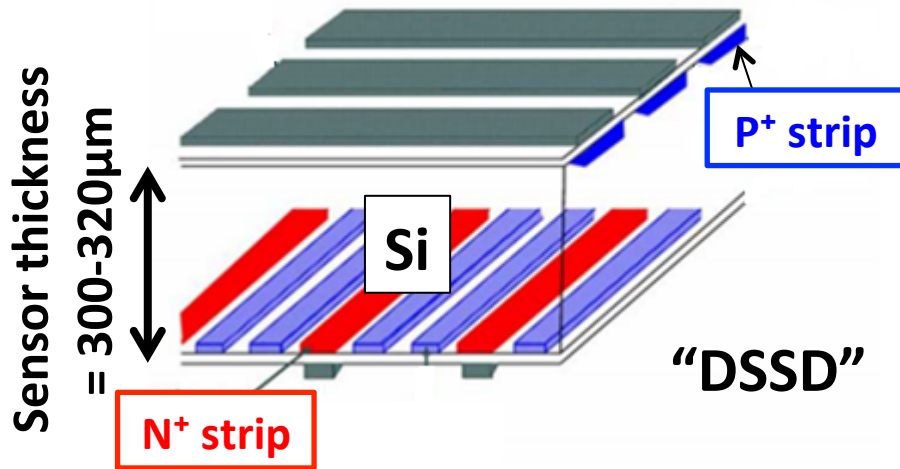
Rectangular sensor



Trapezoidal sensor

SVD Sensors and Readout ASIC

Double-sided Si strip detector

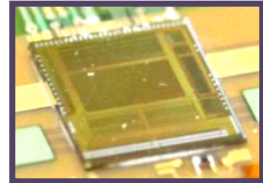


	Rectangular	Trapezoidal
# of <i>p</i> -strips	768	768
<i>p</i> -strip pitch	75µm	50...75µm
# of <i>n</i> -strips	512	512
<i>n</i> -strip pitch	240µm	240µm
Active area	57.72x122.9 mm ²	5890mm ²

Readout ASIC (APV25)

- As high hit rate is anticipated at Belle II, the readout chip should have a short signal shaping time for low noise and a good radiation hardness.

We adopted the APV25

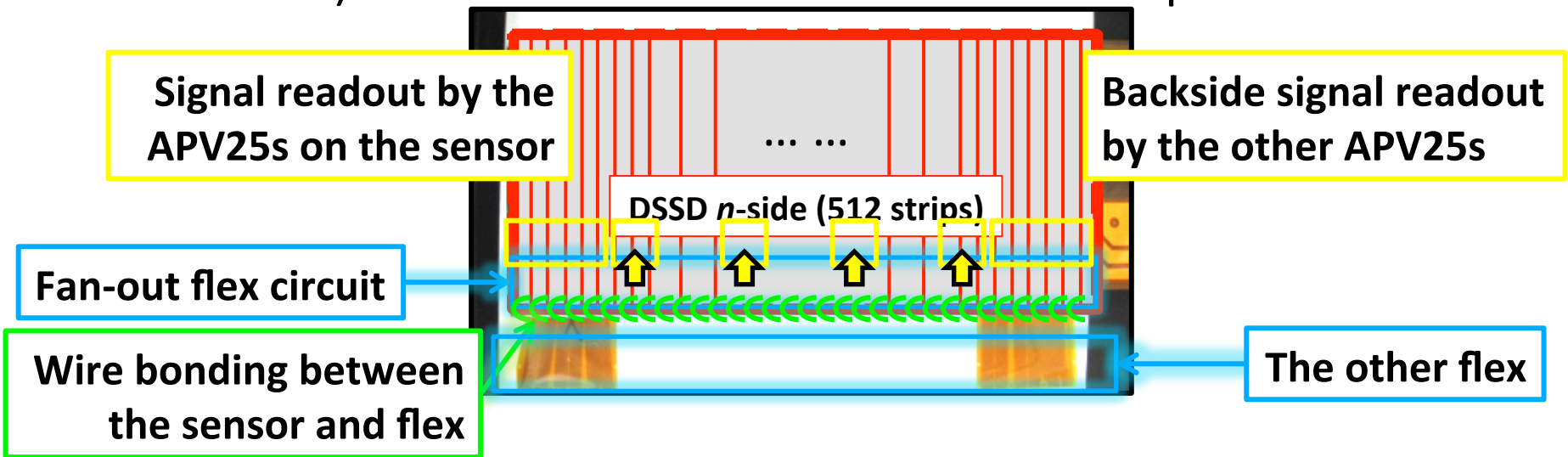


- The APV25 was originally developed for the CMS.
 - **Shaping time = 50ns.**
 - **Radiation hardness > 1MGray.**
- Other characteristics
 - # of input channels = **128 / chip.**
 - **192-deep analog pipeline** for the dead-time reduction.
 - **Thinned down to 100µm** for the material budget reduction.

Chip-on-Sensor and “Origami”

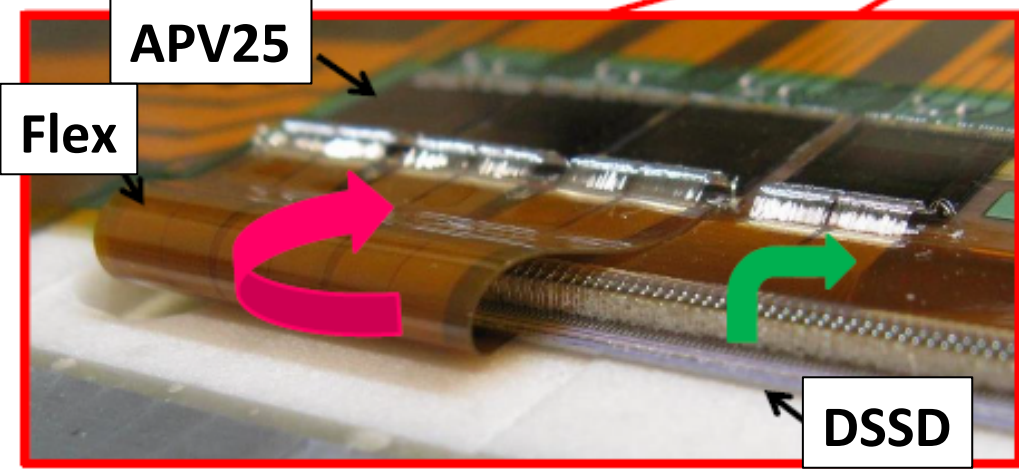
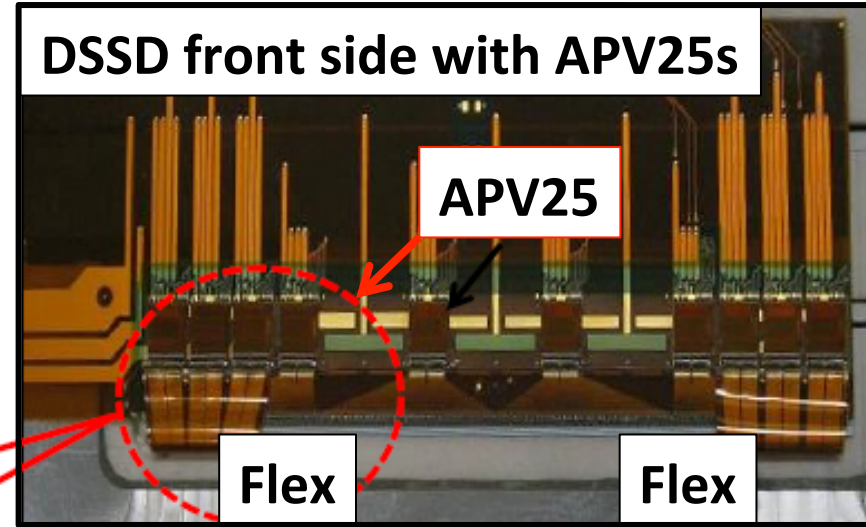
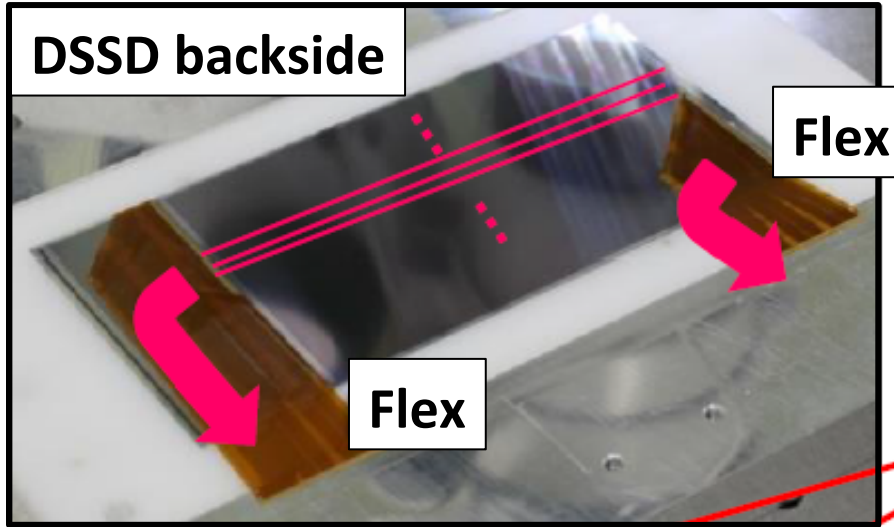
Concepts

- APV25 on sensor
 - The APVs for the inner sensors are placed directly on the DSSDs to minimize the analog path length (capacitive noise)
- P-side readout
 - Signals on the sensor backside are brought to the upper side by other flex circuits and readout by APV25 chips mounted on the top



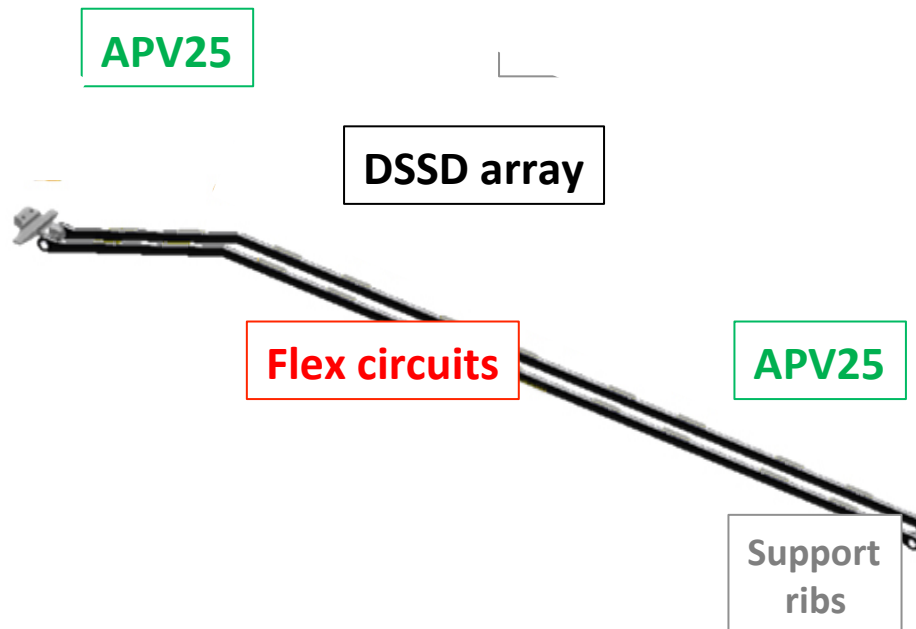
Readout ASICs on the same side & line → easier chilling by a single cooling pipe.

Snapshot – the “Origami” Concept



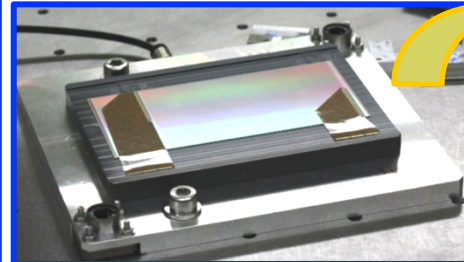
The backside signals are transmitted to the APV25 via bent (and glued) flex circuits.

SVD Ladder Assembly

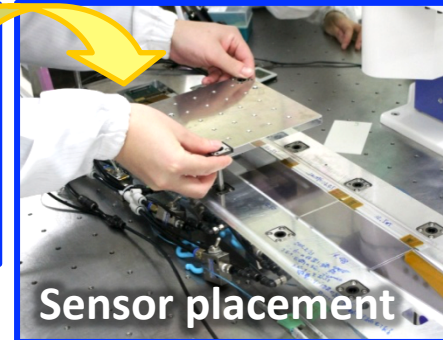


Precision DSSD alignment

DSSDs are handled with precision assembly jigs ($O(50\mu\text{m})$), on which the sensors are fixed by vacuum chucking.

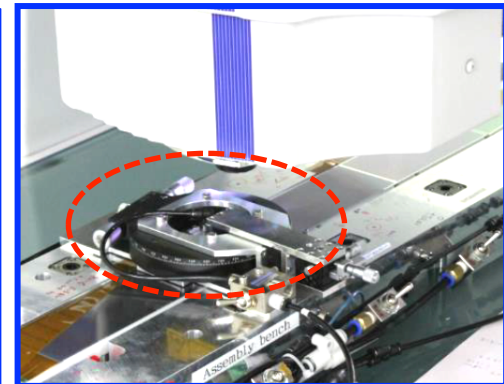


Sensor fixed on a jig



Sensor placement

Sensors are aligned with a Precision of $10\mu\text{m}$ by a position tuning jig with monitoring through a CMM.

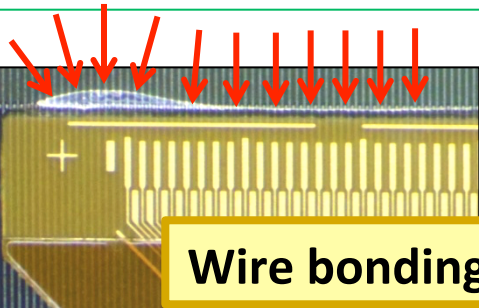


SVD Ladder Assembly

Ladder fabrication: gluing

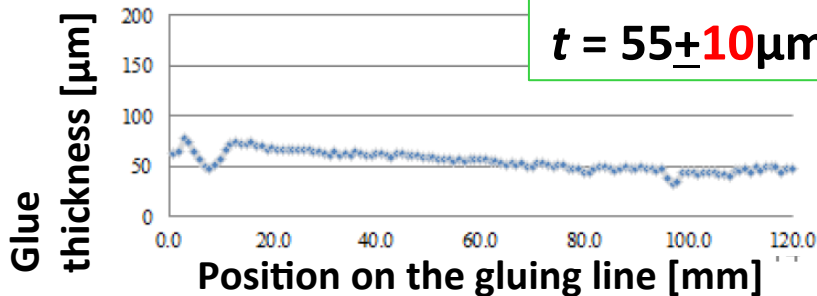
Ladders are fabricated by gluing the components by Araldite®2011

Glue spread below bonding pads can affect the bonding yield and pull strength → glue amount and glue lining are controlled by a gluing robot.



Appropriate spread of glue to the flex edge

Wire bonding pads

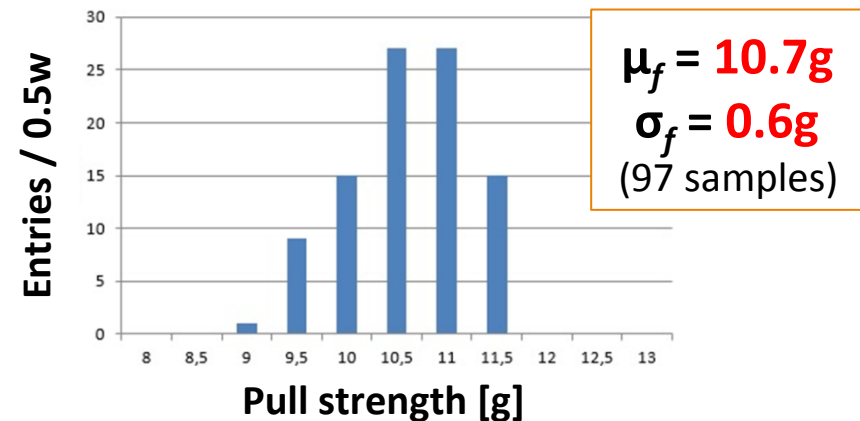


Electrical connection: wire bonding

The flex ↔ DSSD strips and flex ↔ APV25s are electrically connected by the wire bonding with Aℓ(99%) wire ($\phi=25\mu\text{m}$).
Number of total bonds = **450k**.



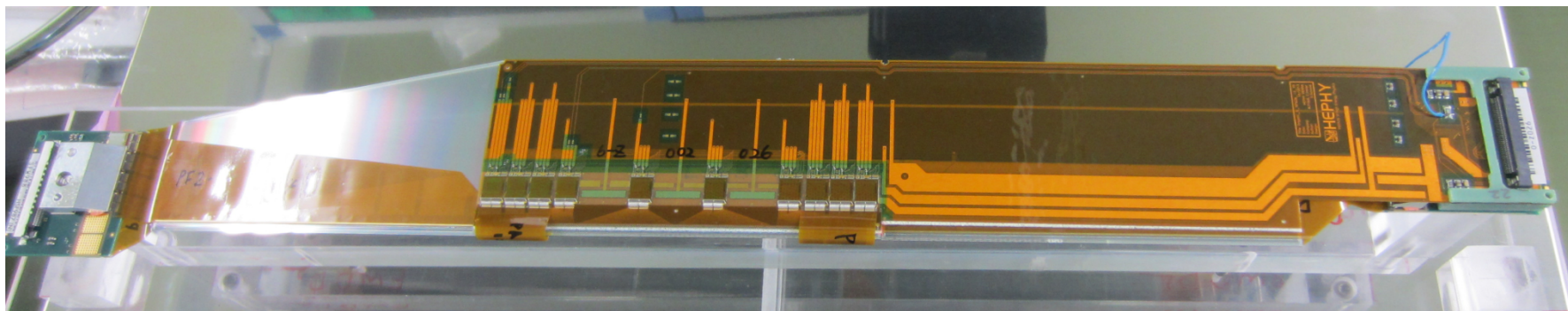
Bonding machine parameters are fine tuned to realize yield >99% and pull strength $f: \mu_f > 5\text{g}$, $\sigma_f / f < 20\%$.



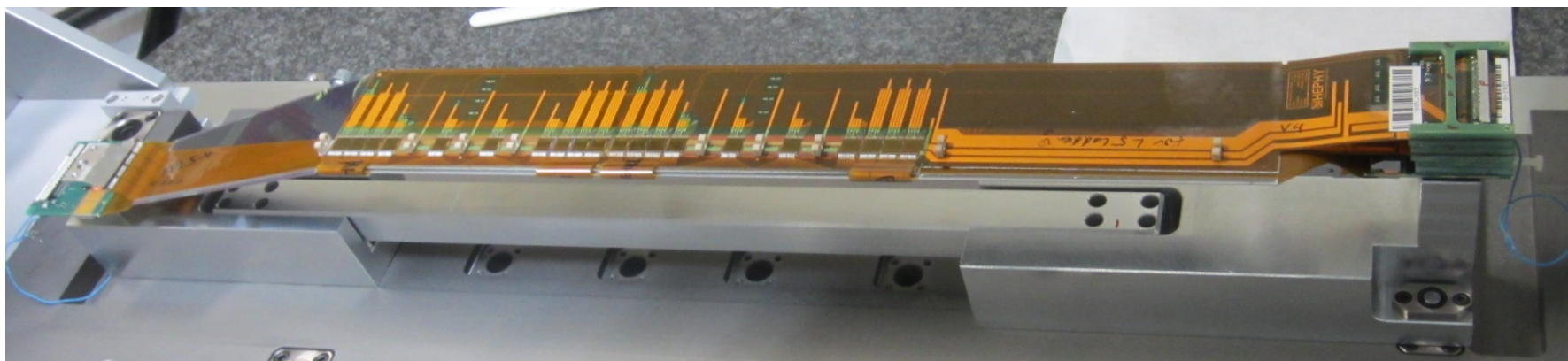
Assembled ladders



L3



L4



L5



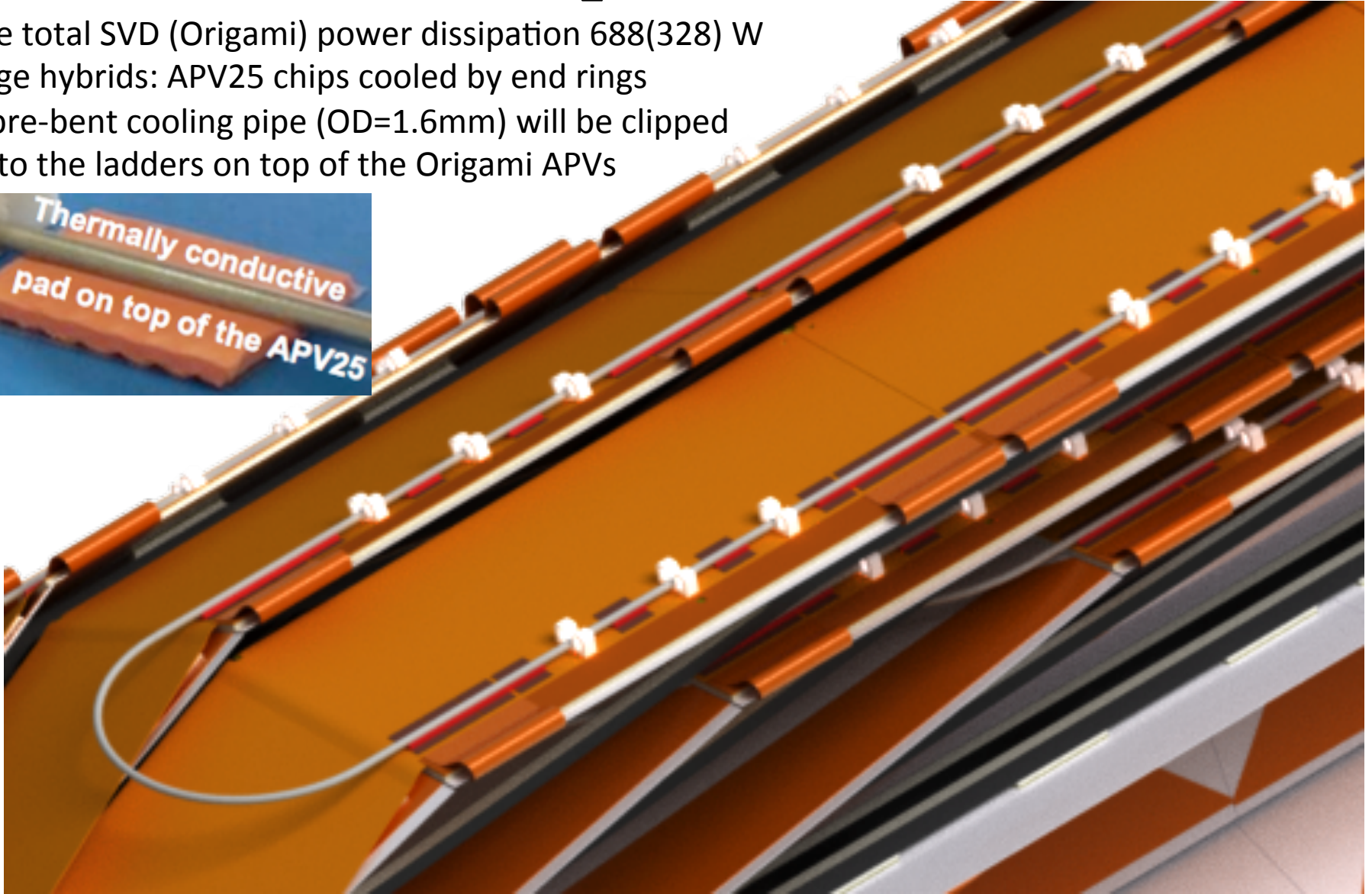
L6

CO₂ Cooling

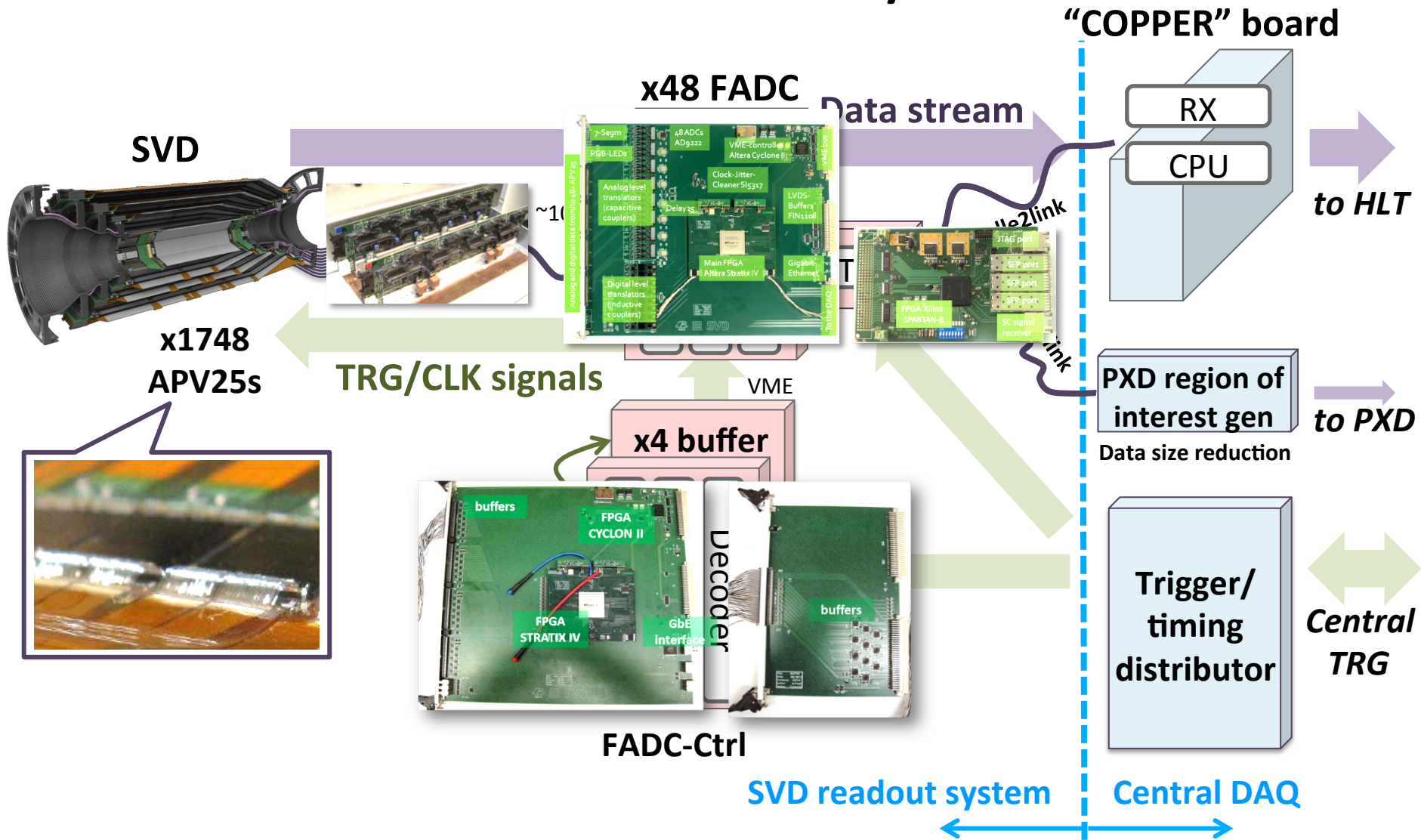
The total SVD (Origami) power dissipation 688(328) W

Edge hybrids: APV25 chips cooled by end rings

A pre-bent cooling pipe (OD=1.6mm) will be clipped onto the ladders on top of the Origami APVs



FADC Readout System



Prototypes of all components have been developed.

Past Reviews

- Class C1 - Onsite review on 5th February 2015
- Class C2 - Onsite review on 27th June 2015
- Class B- (L4.905) - Electrically working but mechanically not
- Class C3 (L4.906) - Mechanically good but one corner of the FW sensor lifted up to 400microns
- L4.905 and L4.906 (remote) - 6th January 2016
- L4.001 (Class B) - 25th February 2016

- ❑ Taking a lead role in the Belle and Belle II experiments in probing NP in the luminosity frontier
- ❑ Both physics and detector (Belle II SVD)